Engineered yeast tolerance enables efficient production from toxified lignocellulosic feedstocks

ENGINEERING

Engineered yeast tolerance enables efficient production from toxified lignocellulosic feedstocks

Felix H. Lam[1,2], Burcu Turanlı-Yıldız[1,2], Dany Liu[1,2†], Michael G. Resch[3], Gerald R. Fink[2]*, Gregory Stephanopoulos[1]*

Lignocellulosic biomass remains unharnessed for the production of renewable fuels and chemicals due to challenges in deconstruction and the toxicity its hydrolysates pose to fermentation microorganisms. Here, we show in *Saccharomyces cerevisiae* that engineered aldehyde reduction and elevated extracellular potassium and pH are sufficient to enable near-parity production between inhibitor-laden and inhibitor-free feedstocks. By specifically targeting the universal hydrolysate inhibitors, a single strain is enhanced to tolerate a broad diversity of highly toxified genuine feedstocks and consistently achieve industrial-scale titers (cellulosic ethanol of >100 grams per liter when toxified). Furthermore, a functionally orthogonal, lightweight design enables seamless transferability to existing metabolically engineered chassis strains: We endow full, multifeedstock tolerance on a xylose-consuming strain and one producing the biodegradable plastics precursor lactic acid. The demonstration of "drop-in" hydrolysate competence enables the potential of cost-effective, at-scale biomass utilization for cellulosic fuel and nonfuel products alike.

INTRODUCTION

Meaningful displacement of greenhouse gas emissions from continued oil consumption requires a renewable feedstock that is transformable into products fungible with petrofuels and petrochemicals and is deployable on a similar scale. Despite the declining cost of carbon-free electricity and rise of emission-free vehicles, studies estimate that this segment will comprise at most 31% of the global fleet by 2040 due to nonroad modes of carriage and long average ownership in the established internal combustion fleet (*1*). As the transportation sector remains the largest generator of carbon dioxide, the sheer number of legacy vehicles necessitates that liquid biofuels play a dominant role in any future energy mix to minimize net emissions (*2*).

Lignocellulosic biomass, the largest renewable terrestrial resource, provides a realistic intermediate-term route to sustainable fuel and nonfuel commodities at enormous scale when paired with suitable fermentation infrastructure (*3*). In addition to quantities on the magnitude of fossil carbon, lignocellulose addresses issues such as food-fuel competition and arable land use that beset present-generation feedstocks such as corn (*4*). Fermented fuel products, notably ethanol, can be blended directly into the gasoline supply at 15 to 85% or chemically dehydrated to ethylene and upgraded into jet fuel (*5*).

However, the severe pretreatments needed to deconstruct the highly recalcitrant plant fibers into fermentable sugars typically result in feedstocks toxic to microorganisms (*6*–*8*). Partly saddled by these technical challenges, the U.S. cellulosic ethanol industry has dwindled sharply (a single preproduction plant run by POET-DSM remains), and pretreatment research has refocused on conversions that yield clarified, biocatalyst-friendly substrates (*9*, *10*). Even then, the greater complexities required by these processes have generally increased costs (estimates as high as 30¢ per gallon ethanol) as well as eroded scalability and competitiveness (*11*). Engineering elevated microbial tolerance to the inhibitors released in simpler, but more aggressive, hydrolytic methods would, therefore, address one of the major obstacles impeding greater utilization of cellulosic feedstocks (*12*–*15*). Here, we show that a targeted combination of genetic and feedstock modifications is sufficient to enhance a single strain to tolerate a wide variety of highly toxified biomass hydrolysates and deliver cellulosic ethanol with performance comparable to current clean sugar ethanol. Our rationally designed approach is, additionally, highly modular: With introduction of a single gene and no further engineering, feedstock-agnostic hydrolysate tolerance is conferred on previously engineered metabolic chassis strains (including one synthesizing a biodegradable plastic) to enable cellulosic products beyond ethanol.

RESULTS

Our prior research demonstrated that in yeast, *Saccharomyces cerevisiae*, responsible for the current global output of biofuel ethanol, increases in media potassium (K^+) and pH were sufficient to strengthen membrane potential and enhance production universally across laboratory and industrial strains (*16*). We, therefore, sought to ascertain the impact of these extracellular adjustments on the fermentation of toxic lignocellulosic feedstocks. Unrefined hydrolysates of all plant biomass, particularly those pretreated under acidic conditions, contain a spectrum of inhibitory by-products but are dominated by the furan aldehydes furfural and 5-hydroxymethylfurfural (HMF) (from dehydration of pentoses and hexoses, respectively) and acetic acid (from deacetylation of hemicellulose) (*17*–*23*).

To systematically characterize the impact of these constituent toxicities, we assessed ethanol production in yeast synthetic complete medium (YSC) with the three inhibitors added individually at equimolar concentration. As a completely chemically defined formulation with trace vitamins, minerals, and amino acids, YSC lacks the

[1]Department of Chemical Engineering, Massachusetts Institute of Technology, Cambridge, MA 02139, USA. [2]Whitehead Institute for Biomedical Research, Cambridge, MA 02142, USA. [3]National Bioenergy Center, National Renewable Energy Laboratory, Golden, CO 80401, USA.
*Corresponding author. Email: gregstep@mit.edu (G.S.); gfink@wi.mit.edu (G.R.F.)
†Present address: Department of Biology and Biological Engineering, Chalmers University of Technology, Göteborg, Sweden.

undefined extracts contained in "rich" media that could supply unknown components to boost or hinder tolerance. A diploid prototroph of laboratory strain S288C was used to preclude nutrient liabilities, and fermentations were conducted for 48 hours at 30°C under high pitch [cell density of optical density at 600 nm (OD_{600}) = 20] and high gravity (250 g/liter of glucose) conditions to mimic industrial production (*24*). Compared to an ethanol titer of 64 ± 0.2 g/liter in unmodified YSC, the presence of 100 mM acetic acid (green outline), furfural (purple outline), or HMF (brown outline) reduced production respectively to 17 ± 0.1, 4 ± 0.3, and 34 ± 0.3 g/liter, establishing furfural as the most deleterious component (Fig. 1A, gray) (*25*). On the basis of our prior tolerance research, we supplemented each with 50 mM potassium chloride (KCl) and ammonium hydroxide (NH_4OH) to achieve pH 6 and observed widely varying recoveries (Fig. 1A, dark blue). For acetic acid, these additions restored production to 109 ± 0.6 g/liter, effectively matching that of K^+/pH-elevated YSC. The prevalence of acetate salt at pH values sufficiently above its pK_a of 4.76 (where K_a is the acid dissociation constant) completely abolished toxicity and, over a concentration range applicable to genuine hydrolysates, the salt was fully tolerated by yeast (fig. S1A) (*17*, *26*). Moreover, supplementation solely with KCl provided no amelioration, demonstrating that acetic acid tolerance arises entirely from acid neutralization (Fig. 1A, light blue).

Elevated K^+ and pH also conferred improvements to furfural and HMF but to titers substantially below that of equivalently elevated YSC. On the basis of our prior work that delineated a mechanism of multialcohol tolerance, these improvements, however small, were unlikely to have arisen from tolerance elicited to the 4 ± 0.3 or 34 ± 0.3 g/liter of ethanol produced under inhibition (*16*). Rather, given reports that *S. cerevisiae* has various dehydrogenases sufficiently promiscuous to reduce furfural and HMF, we surmised that these extracellular adjustments were conferring tolerance to their furan alcohol products (*27*–*30*). We detected 2-furanmethanol (FF-OH) and furan-2,5-dimethanol (HMF-OH) in significant amounts ($P \leq 3.35 \times 10^{-5}$), along with the disappearance of furfural and HMF, after only 24 hours of fermentation [Fig. 1B, wild type ("WT")]. When comparing the relative toxicity imposed by these alcohols versus their aldehyde equivalents, an ethanol output of 35 ± 0.4 g/liter demonstrated that FF-OH was 9× more tolerated than furfural at equimolar concentration (pink versus purple outline, gray); with extracellular adjustments (pink outline, dark blue), production was boosted an additional 69% to 59 ± 0.5 g/liter (Fig. 1A). The same trend was recapitulated with HMF where HMF-OH accorded 45% higher titer (beige versus brown outline, gray), and media modifications yielded a further 39% that corresponded to production of 69 ± 0.6 g/liter (beige outline, dark blue). Unlike acetic acid where K^+-only supplementation showed no improvement,

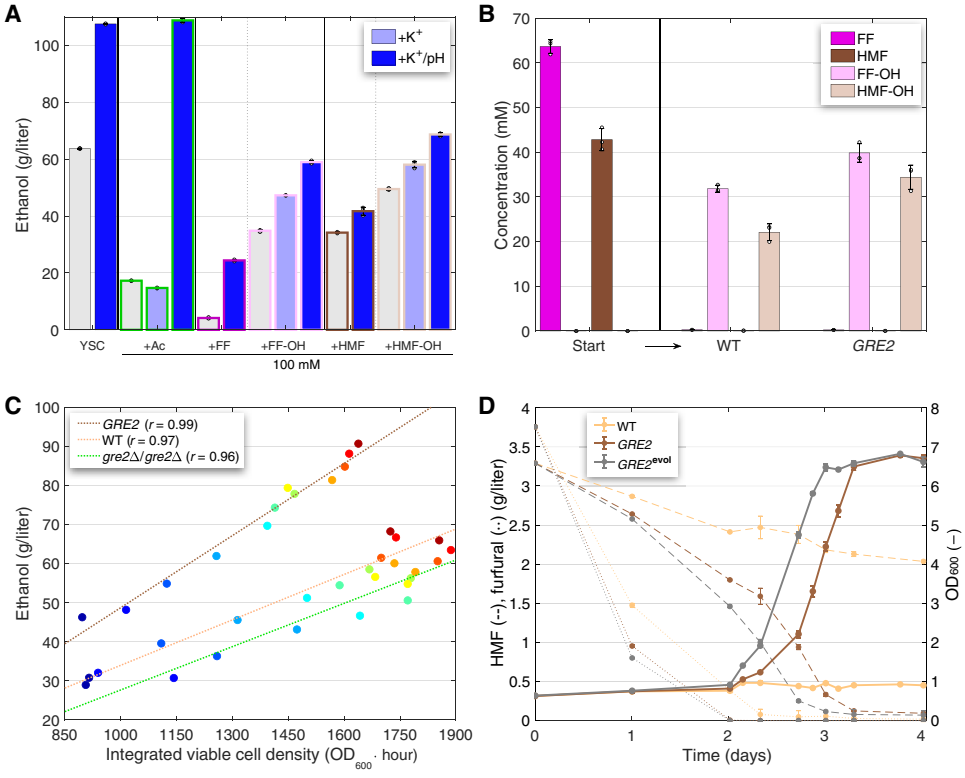

Fig. 1. Elevated extracellular K^+ and pH combined with *GRE2* overexpression confer tolerance to lignocellulosic hydrolysate toxicity. (**A**) Ethanol titers from the prototrophic wild-type (WT) fermenting synthetic medium containing the indicated additions: green outline, acetic acid (Ac); purple outline, furfural (FF); pink outline, FF-OH; brown outline, HMF; beige outline, HMF-OH; K^+, 50 mM KCl; K^+/pH, 50 mM KCl and NH_4OH to pH 6. (**B**) Quantification of the indicated species in medium containing elevated K^+ and pH buffering, toxified with the benchmark suite of furfural, HMF, and acetic acid, and measured after 24 hours of fermentation in the WT or *GRE2* overexpression strain. (**C**) Ethanol titers correlated with time integrals of viable cell densities from toxified medium containing increasing K^+ and/or pH by the *GRE2* overexpression strain, WT, or *gre2*Δ/*gre2*Δ deletion strain. (**D**) Cell growth, and furfural and HMF depletion, in toxified medium by the WT, *GRE2* overexpression strain, or *GRE2*^{evol} overexpression strain. Data are means ± SD from three biological replicates.

the addition of KCl alone to FF-OH and HMF-OH (pink and beige outline, light blue) elicited improvements intermediate to those with KCl and NH_4OH together. This behavior was consistent with that observed previously for ethanol and underscored the specificity of the membrane permeabilization, and K^+/pH countermeasures, to alcohol toxicity (*16*). Furthermore, across concentrations relevant to genuine hydrolysates, these adjustments consistently elicited an enhancement, one whose efficacy was sustained over a larger range with FF-OH and HMF-OH than with furfural and HMF (fig. S1, B and C). Given the gains attainable individually on the three dominant inhibitors, we surmised that augmenting in vivo conversion of furfural and HMF to alcohols, paired with the elevation of extracellular K^+ and pH, could encapsulate a unified method for bestowing tolerance against the totality of toxicities present in genuine hydrolysates.

On the basis of literature describing reductases with detoxifying activity toward furfural and HMF, we constructed yeast strains overexpressing *ADH6*, *ADH7*, or *GRE2* from *S. cerevisiae* or *ADH4* from *Scheffersomyces stipitis* (*29*–*33*). Fermentation benchmarking over two repressive conditions combining the trio of inhibitors revealed that *S. cerevisiae GRE2* evoked the greatest improvement among the candidates. When compared to the WT, these improvements amounted to as much as 32% (fig. S2). Furthermore, that the *GRE2* strain sustained a smaller production drop than the WT under the harsher of the two conditions suggested that increased detoxification can enhance robustness over a wider range of toxicity. We quantified FF-OH and HMF-OH to corroborate the augmented reduction capacity and found that *GRE2* overexpression produced 25 ± 1% higher concentrations of FF-OH and 56 ± 6% of HMF-OH ($P \leq 3.2 \times 10^{-3}$; Fig. 1B "*GRE2*"). Despite nonstoichiometric conversion of furfural and HMF, that greater formation of FF-OH and HMF-OH could be engineered indicated that we could indeed productively mitigate the aggregate toxicity by converting the aldehydes into a form (alcohols) for which we have the means to counteract effectively.

To characterize productivity under combined furfural and HMF stress, as well as the impact from modulating reductase activity, we quantified the relationship between tolerance and ethanol production for the WT, the *GRE2* overexpression strain, and one deleted for *GRE2*. Our prior work had demonstrated that the viable fraction in an actively fermenting population declined rapidly with accumulating ethanol; however, this mortality could be rescued by K^+ and pH adjustments in a dose-dependent manner. Furthermore, time integrations of these viable population measurements ("integrated viable cell density") from progressively higher adjustments, followed by correlation with ethanol titers, established the relationship between tolerance and production. Specifically, a readout of the time-averaged specific productivity exclusive to the differentially decaying viable fractions was revealed in the correlation slope (*16*). We, therefore, measured titers and viabilities from a series of fermentations containing furfural, HMF, and incrementally higher adjustments of K^+ and/or pH. The slope from the *GRE2* strain revealed a 59% improvement in per-cell performance over the WT, demonstrating that increased detoxification subdued the combined inhibition effectively to sustain metabolic activity (Fig. 1C). For higher extracellular adjustments (e.g., yellow to red data points), we quantified the *GRE2* strain to actually have lower viabilities yet greater ethanol production, illustrating that WT cells, while alive, were stalled metabolically (fig. S3). Furthermore, the higher prevalence of alcohols from *GRE2* overexpression (from HMF-OH and FF-OH formation as well as improved ethanol production) likely predisposed the strain to the increasing alcohol protective benefits of incremental K^+ and pH, the outcome of which was reflected as higher per-cell performance. Deletion of *GRE2* corroborated these trends: While the *gre2Δ*/*gre2Δ* strain retained the same specific productivity as the WT, the downshift in correlation indicated that any given viability or particular extracellular adjustment would result in lower ethanol output. Thus, *GRE2* contributes directly to the resilience of the population by converting furfural and HMF aldehyde stress into alcohols that are subsequently ameliorated by K^+ and pH treatment.

Given the efficacy exhibited by the *GRE2* overexpression strain, we considered various adaptation approaches to further improving hydrolysate tolerance. While whole-strain laboratory adaptive evolution is well practiced for augmenting fitness, selective advantages from genome-wide drift have been shown to incur costs in robustness (*34*, *35*). To minimize the risk of pleiotropic deficits undermining feedstock range and strain performance, we opted to hone the detoxification capabilities of *GRE2* specifically via directed evolution. Therefore, we cultured a yeast library consisting of polymerase chain reaction (PCR)–mutagenized *GRE2* variants under combined furfural, HMF, and acetic acid stress and challenged it to increasing loads over time (fig. S4) (*36*). Validated, postselection sequence isolates were subcloned and introduced anew into S288C, and individual strains screened for a fermentation advantage.

The allele exhibiting the greatest gain was a triple mutant containing a proline to serine substitution at amino acid 48, isoleucine to valine at amino acid 290, and a silent aspartate mutation at amino acid 133 ($GRE2^{P48S + I290V + D133D}$; hereafter as $GRE2^{evol}$). Across several toxicity combinations mimicking a range of pretreatment severities, $GRE2^{evol}$ consistently conferred improvements over unevolved *GRE2* in ethanol production (fig. S5A). Other than K^+ and pH requirements, the superior phenotype was not dependent on extracellular factors supplied by a favorable nutritional environment: In yeast nitrogen base (YNB) minimal medium, containing no amino acids and solely glucose, ammonium sulfate, salts, and trace vitamins, $GRE2^{evol}$ was capable of eliciting a percentage gain comparable to those observed under nutrient-replete conditions (fig. S5B). Furthermore, under nontoxic conditions where the superphysiological abundance and reductive capacity of $GRE2^{evol}$ could potentially cross-react with acetaldehyde to boost ethanol yield, we observed statistically unchanged levels of performance (fig. S5C). Along with the absence of a major negative impact, these data suggested that the highly transcribed $GRE2^{evol}$ imposed a low-expression burden and functioned largely in an orthogonal manner specific to the hydrolysate inhibitors.

As rates of detoxification are directly proportional to cell biomass (Fig. 1B demonstrated that even the WT could completely reduce furfural and HMF in under 24 hours at production cell densities), we lowered inocula more than 20× in a growth assay designed to emphasize fitness advantages enabled by $GRE2^{evol}$ under full toxicity. Here, the WT failed completely to expand, while $GRE2^{evol}$ shortened the lag phase by approximately 7 hours compared to overexpressed unevolved *GRE2* (Fig. 1D). The exit from lag was preceded by the detoxification of furfural and HMF, where $GRE2^{evol}$ exhibited the highest rates of depletion. Incidentally, when juxtaposed with growth, the decreases in inhibitor concentration revealed further that, unlike furfural, HMF need not be fully detoxified in order for growth to commence and approximately 1.5 g/liter are tolerable by yeast.

Expression of *GRE2*^{evol} was, moreover, capable of conferring near-parity ethanol production between inhibitor-free and fully toxified conditions. To first establish a reference upper bound for inhibitor-free productivity and titer, we fermented the WT in traditional high glucose synthetic medium supplemented with potassium bicarbonate ($KHCO_3$) and calcium carbonate ($CaCO_3$), selected for their widespread industrial and agricultural availability, to provide elevated K^+ and pH buffering. Under these optimal conditions, ethanol reached 109 ± 1 g/liter in under 32 hours (Fig. 2A, blue). When we proceeded to toxify with 62 mM furfural, 48 mM HMF, and 100 mM acetic acid, a benchmark of above-average toxicity that we formulated to balance broad feedstock applicability with acceptable yeast performance, output was repressed by 69% to 34 ± 1.2 g/liter of ethanol. This was despite the adjustment to pH 5 per standard bioethanol practices that also neutralized the acetic acid component (Fig. 2A, red) (*17*, *18*, *21*, *37*). Subsequent supplementation with $KHCO_3$ and $CaCO_3$ was sufficient to rescue stalled productivity in the WT and achieve production of 81 ± 2 g/liter (Fig. 2A, orange). However, substitution with the *GRE2*^{evol} strain provided a further gain, boosting rate by an additional mean 39% and final product by 31% (Fig. 2A, gray solid). The ethanol titer of 106 ± 1 g/liter amounted to 97% of that from inhibitor-free medium, demonstrating near-unrestricted ethanol production under full toxicity conditions. Moreover, that the *GRE2*^{evol} strain remained predominantly repressed under toxification at pH 5 (Fig. 2A, gray dotted) illustrated the necessity of both the genetic- and extracellular-derived enhancements to attain maximal tolerance.

The targeted detoxification provided by the combination of *GRE2*^{evol} expression and feedstock adjustments was applicable beyond artificial formulations to a range of genuine lignocellulosic feedstocks. Influenced partly by their history of toxicity and limited utility, the hydrolysates currently available are produced largely at research scale and focused on maximally detoxified cellulosic sugars (*6*–*8*, *10*, *38*, *39*). We procured a collection of seven samples representing a diversity of plant sources (corn stover, sugar cane bagasse, wheat straw, giant miscanthus, and switchgrass) and various pretreatment methods and confirmed that inhibitors were present in the ranges of 0.1 to 21 mM furfural, 0.1 to 6 mM HMF, and 0 to 178 mM acetic acid (table S1). These quantities were sufficiently mild such that, aside from the standard supplementation with urea (to provide nitrogen) and adjustment to pH 5, the WT was capable of fermenting all glucose to completion under otherwise unmodified conditions (Fig. 2B, blue, and fig. S6).

Because inhibitor and glucose loads inherent in most of the samples fell below that of our formulated benchmark, we toxified all samples to impinge on our engineered tolerance limits (table S2). Furfural was raised to an average of 45 mM, HMF to 35 mM, and acetic acid to 100 mM to more closely align with published inhibitory combinations, and glucose was raised to an average of 220 g/liter for increased osmotic, and ensuing ethanol, stress (*17*–*23*). Supplementation with pure chemical forms of these components was necessary as prehydrolyzed solids (and hydrolysis methods) were unavailable to us to boost toxicity using raw cellulosic material. Under these conditions, the WT became repressed even with adjustments to pH 5 (Fig. 2B, red). In deacetylated and mechanically refined (DMR) corn stover, for example, this repression amounted to an output 39% of its minimally modified control. (Glucose supplementation in the remaining feedstocks concomitantly raised ethanol ceilings, rendering comparisons with their minimally modified, lower-glucose controls invalid). The subsequent

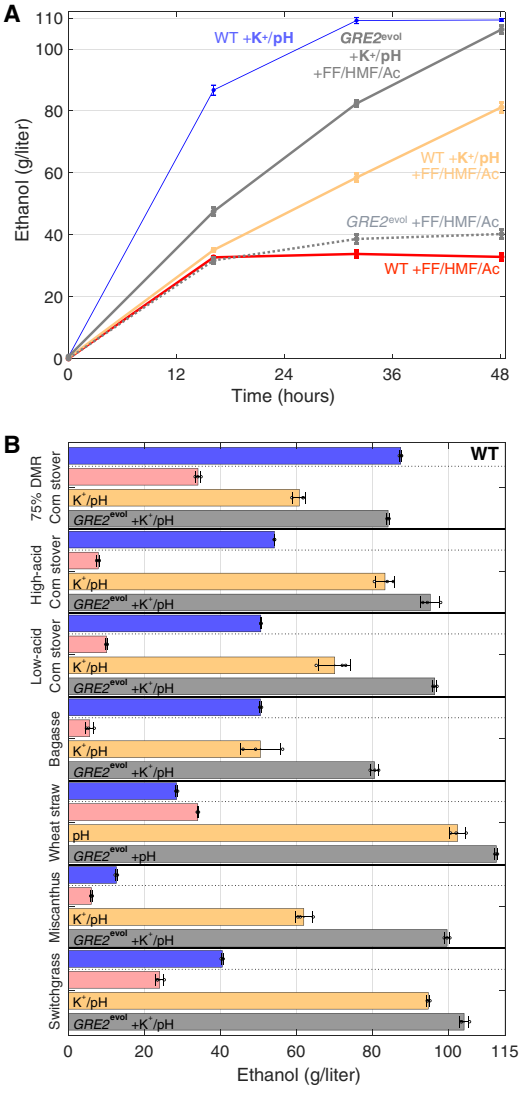

Fig. 2. Elevated K^+, pH buffering, and *GRE2*^{evol} overexpression enable near-parity ethanol production between inhibitor-free and fully toxified conditions and confer robustness across diverse feedstocks. (**A**) Ethanol production from the WT fermenting synthetic medium supplemented solely with potassium and carbonate buffer (blue); toxified with the benchmark suite of furfural, HMF, and acetic acid and adjusted to pH 5 (red); toxified with the benchmark suite of furfural, HMF, and acetic acid but supplemented with potassium and carbonate buffer (orange); same as orange but fermented with the *GRE2*^{evol} strain (gray solid); and same conditions as red but fermented with the *GRE2*^{evol} strain (gray dotted). (**B**) Cellulosic ethanol titers from biomass hydrolysates where blue is minimally modified feedstock (urea and adjusted to pH 5 if needed); red is toxified with furfural, HMF, acetic acid, and glucose (except no additional glucose in DMR corn stover), supplemented with urea, and adjusted to pH 5 if needed (inhibitor concentrations in table S2, white columns); orange is the same as red but adjusted with potassium and carbonate buffer in lieu of base addition to pH 5 (table S2, white and gray columns); and gray is identical to orange but fermented with the *GRE2*^{evol} strain. Data are means ± SD from three biological replicates.

addition of K^+ and pH buffering elicited increases of 1.8 to 10.7×, enabling 57 to 91% of the previously residual glucose to be consumed (Fig. 2B, orange, and fig. S6). However, when these additions were combined with the *GRE2*^{evol} strain, over 91% of the final remaining substrate was consumed, increasing production by 10 to

61% over the WT to titers of 81 ± 1 to 113 ± 0.4 g/liter (Fig. 2B, gray, and fig. S6). This performance corresponded to theoretical conversion yields of 78 to 91% and were all obtained from a single strain derived from a historically underperforming laboratory lineage; yet, they exceeded currently published values of cellulosic ethanol produced from undetoxified industrial feedstocks (*40*–*42*). Thus, despite the compositional and pretreatment–by-product complexity across this diversity of material (e.g., miscanthus contains ferulic and *p*-coumaric acids derived from lignin degradation; table S3), the combination of *GRE2*^{evol} and alcohol protective adjustments exhibited robustness and sufficiency to efficiently ferment highly toxified genuine feedstocks.

Because genuine hydrolysates are highly undefined mixtures with unknown levels of salts, uninformed additions of K^+ and particular buffer countercations could potentially exceed osmotic shock thresholds in yeast (*43*–*45*). As we had previously established fermentation-beneficial effects of K^+ to at least 110 mM and Ca^{2+} to be fermentation neutral, we deemed it important to maintain total K^+ within this limit and modulate pH via Ca^{2+}-based buffers or bases (*16*). Thus, cation concentrations in each sample were determined by mass spectrometry and used to determine the specific mixes of $KHCO_3$, $CaCO_3$, and calcium hydroxide to provide as supplementation (tables S1 and S2). The atypically high K^+ concentration in wheat straw provided an opportunity to validate these constraints: When 50 mM $KHCO_3$ and 100 mM $CaCO_3$ were used in lieu of 150 mM $CaCO_3$, the oversupply of K^+ resulted in decreases to performance despite the same buffering capacity (fig. S7). Therefore, supplementation customized to each feedstock conforming to salt-specific limits is necessary to achieve maximal efficacy.

These tolerance capabilities were fully transferrable to the fermentation of inhibitor-laden xylose, the pentose comprising a substantial portion of lignocellulosic sugars that unmodified *S. cerevisiae* cannot consume (*6*, *17*). Our laboratory had previously engineered a strain (*XYL*$^+$) that efficiently fermented xylose to ethanol but preferentially used glucose if present (*46*). Therefore, we formulated a YSC-based hydrolysate to favor xylose metabolism, yet mimic genuine cellulosic proportions, by combining xylose with starch whose glucan polymers were slowly digested to glucose via incrementally dosed amylases. In the absence of inhibitors, the *XYL*$^+$ chassis completely consumed available xylose and glucose in this medium and produced 62 ± 0.9 g/liter of ethanol (Fig. 3A, bold blue, and fig. S8). Toxification with the benchmark suite of furfural, HMF, and acetic acid repressed production to 8 ± 1 g/liter, and subsequent treatment with elevated K^+ and pH buffering provided recovery to 22 ± 0.9 g/liter with improved proportional usage of sugar (Fig. 3A, bold red and orange, and fig. S8). However, when we introduced *GRE2*^{evol} into *XYL*$^+$ with no further modifications, the chassis was functionalized to ferment all xylose and glucose, restoring production essentially 100% to 66 ± 0.6 g/liter (Fig. 3A, bold gray, and fig. S8). Our combination of tolerance enhancements thus liberated the prior-engineered metabolism to achieve full production capacity under complete toxicity conditions.

Moreover, the *GRE2*^{evol}-enhanced *XYL*$^+$ strain maintained its tolerance capabilities on multiple toxified genuine hydrolysates. Because of catabolite repression, xylose went unconsumed by the *XYL*$^+$ chassis strain in minimally modified hydrolysates of sugarcane bagasse and high-acid corn stover (Fig. 3A, nonbold blue, and fig. S8). Miscanthus proved, fortuitously, to be an exception: As glucose was present in amounts lower than xylose and depleted rapidly,

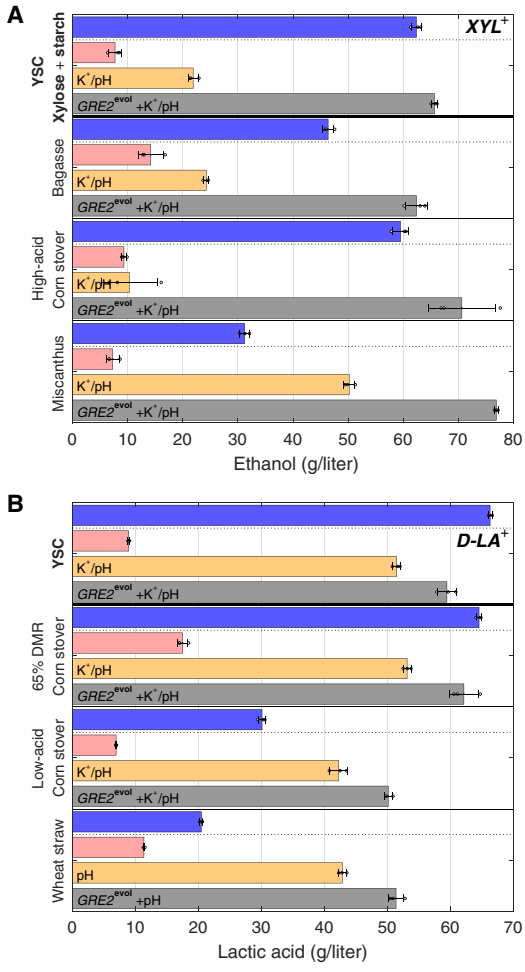

Fig. 3. Elevated K^+, pH buffering, and *GRE2*^{evol} overexpression encapsulate a lightweight cellulosic tolerance platform integrable with heterologous engineered pathways. Bars follow the conditions and color scheme described in Fig. 2B. (**A**) Cellulosic ethanol titers from a xylose-consuming strain (*XYL*$^+$) fermenting synthetic medium (bold) containing xylose and starch (slowly hydrolyzed to glucose via amylases), or the indicated biomass hydrolysate (nonbold). (**B**) Cellulosic lactic acid titers from an ethanol-handicapped strain expressing lactate dehydrogenase from *L. mesenteroides* (D-*LA*$^+$) fermenting synthetic medium (bold) or the indicated biomass hydrolysate (nonbold). Data are means ± SD from three biological replicates.

xylose metabolism remained sufficiently active such that both monomeric sugars were near-entirely consumed. Toxification from increased glucose, furfural, HMF, and acetic acid repressed production in all three hydrolysates to below 15 g/liter of ethanol. While these inhibitory conditions were relieved by elevated K^+ and pH buffering, the recoveries exhibited much greater variability than in S288C (Fig. 3A, nonbold red and orange, and table S2). In high-acid corn stover, for example, an improvement was statistically questionable (P = 0.76), while that for miscanthus was a significant 689 ± 1% ($P = 1.00 \times 10^{-6}$). However, these inconsistent recoveries were subsequently remedied in a robust manner by the introduction of *GRE2*^{evol} where gains averaged a further 260% (Fig. 3A, nonbold gray). In miscanthus, this additionally enabled partial fermentation of xylose despite higher catabolite repression from supplemented

glucose (fig. S8). Again, our combination genetic and extracellular tolerance enhancements proved effective across disparate toxified genuine feedstocks.

The recapitulation of phenotype and substrate robustness on a preexisting metabolic chassis suggested that *GRE2*^{evol} expression and K^+/pH feedstock adjustment could constitute a functionally orthogonal tolerance platform integrable with other engineered end products. Given that our alcohol-focused countermeasures may have conferred a bias toward ethanol production, we opted to endow hydrolysate tolerance on a glucose-consuming strain synthesizing the biodegradable plastics precursor lactic acid (D-LA), a chemical commodity projected to reach U.S. $9 billion by 2025 (*47*). Given the evolutionary predilection of *S. cerevisiae* for alcoholic fermentation, elimination of ethanol has been a major goal in all efforts to reengineer yeast for nonethanol products. Here, we opted to minimize, rather than eliminate, glycolytic flux toward ethanol to maintain subsistence adenosine 5′-triphosphate generation for cell growth and active lactate export (*48*). As lactate and ethanol share a common precursor in pyruvate, we curtailed pyruvate decarboxylase activity and losses to ethanol by creating a *pdc1*Δ/*pdc1*Δ *pdc5*Δ/*pdc5*Δ::p*TEF1*m4-*PDC5* strain where a sole chromosomal pyruvate decarboxylase gene was transcribed using a handicapped variant of the *TEF1* promoter (*49*–*51*). Reductive conversion of pyruvate to lactate was fulfilled via expression of D-lactate dehydrogenase from *Leuconostoc mesenteroides* (*52*).

In synthetic medium supplemented with $KHCO_3$ and sufficient $CaCO_3$ to buffer lactic acid accumulation, and likewise in DMR corn stover minimally supplemented with $CaCO_3$, our *D-LA*$^+$ chassis generated inhibitor-free reference titers of 66 ± 0.3 and 65 ± 0.4 g/liter, respectively (Fig. 3B, blue). Under complete toxification, elevated K^+ and pH buffering, combined with *GRE2*^{evol} expression and no additional modifications, succeeded in conferring tolerance such that cellulosic lactic acid reached 90 and 96% of these clean sugar benchmarks (Fig. 3B, gray). Similar to *XYL*$^+$, the engineered *D-LA*$^+$ metabolism was largely liberated from inhibition to elicit near-unrestricted production. Furthermore, we tested for strain robustness to additional hydrolysates using low-acid corn stover and wheat straw. As before, these feedstocks (unlike DMR corn stover) contained the stress from supplemented glucose and toxification from the trio of inhibitors. Nevertheless, *GRE2*^{evol} expression was capable of eliciting mean gains of 19% over the unengineered chassis to attain cellulosic product titers greater than 50 g/liter.

Although higher lactic acid production from yeast has been reported, all prior studies were conducted using traditional, clean sugar feedstocks; titers here, furthermore, were restrained by our chassis' inherently limited synthesis capabilities (*52*–*54*). The single-transformation tolerance phenotype minimally interfered with the engineered lactic acid metabolism (fig. S5C); likewise, *GRE2*^{evol} remained predominantly orthogonal and unperturbed to alleviate toxicity efficiently. To our knowledge, this represented the first demonstration of a nonethanol cellulosic product delivered with industrially relevant performance from multiple highly toxified genuine feedstocks using a single strain.

DISCUSSION

Our results describe a functionally independent, lightweight platform that both endows yeast with general lignocellulosic hydrolysate tolerance and integrates harmoniously with preexisting metabolically engineered chassis strains. Through systematic characterization of the three dominant toxicities released from biomass pretreatment, we have demonstrated that tolerance to each inhibitor can be realized through standard neutralization (for acetic acid) or conversion of the aldehydes to alcohols, which are subsequently ameliorated by the prior-identified elevated K^+ and pH treatment (for furfural and HMF). The general practice of hydrolysate tolerance can, therefore, be reduced to two specific and readily modifiable parameters: In a genetic background enhanced by *GRE2*^{evol} for the accelerated reduction of furfural and HMF, a large diversity of feedstocks, regardless of plant source and/or pretreatment process, can be accommodated via tailored adjustment of K^+ and pH. This substrate robustness indicates that the spectrum of hydrolytic by-products other than furfural, HMF, and acetic acid (for example, the various acidic and phenolic inhibitors shown in table S3) may be qualitatively immaterial.

These benefits, collectively, renew and boost the value proposition of cellulosic fermentation. Wide feedstock compatibility can reduce the dependence on specific crop types or pretreatments and, consequently, ameliorate the supply variability (e.g., from seasonality, storage stability) and cost uncertainties surrounding biomass (*13*). Similarly, heightened tolerance, in addition to harnessing toxic sugar streams or transport-friendlier concentrates, enables production conditions of minimized contaminant growth that would otherwise require the standard-practice, but public health-concerning, use of antibiotics (*55*). Last, the targeted specificity of our detoxification approach underlies the high decoupling with metabolism and straightforward integration with previously engineered pathways such as those for xylose consumption and lactic acid synthesis. This underscores the notion of a "drop-in" tolerance phenotype extensible to even more non-native capabilities and high-volume biofuels and biochemicals.

MATERIALS AND METHODS

Plasmid construction

All plasmids were assembled using the Gibson method from segments generated via PCR. Amplification of plasmid backbone, yeast promoter, protein coding, and transcription termination fragments (see below) was carried out using the Phusion High-Fidelity DNA Polymerase (New England Biolabs, #M0530; www.neb.com) in 50 μl of reaction following the manufacturer's directions. Primers were designed with 25- to 30–base pair (bp) 5′ overhangs to serve as assembly junctions and annealing temperatures of primer pairs optimized using the vendor-provided calculator (tmcalculator.neb.com). The suggested extension times of 30 s/kb were often inadequate empirically and extended to 60 s/kb for problematic amplicons (fragments of >2 to 3 kb tended to require the higher extension rate). For templates containing a bacterial origin of replication (e.g., plasmid backbone segment), PCR products were further digested with 20 U of Dpn I (New England Biolabs, #R0176) added directly to the reaction sample after thermocycling (i.e., no additional restriction enzyme buffer), incubated for 90 min at 37°C, and heat-inactivated for 20 min at 80°C. All fragments were purified and concentrated (up to three pooled PCR reactions per column) using the QIAquick PCR Purification Kit (QIAGEN, #28106; www.qiagen.com), and DNA concentrations were quantified with a NanoDrop Microvolume ultraviolet-visible spectrophotometer. Gibson reactions were prepared from these eluates using 50 to 100 ng of vector and molar ratios of one part vector to four to eight parts of each insert

in the lowest volume possible (i.e., no additional H_2O to meet the instructed minimum of 10 μl). Assembly enzymes were supplied through a cocktail (New England Biolabs, #E2611), and reactions were incubated for 30 min at 50°C, followed by an additional 1 hour to overnight at room temperature. Chemically competent *Escherichia coli* (New England Biolabs, #C2992) were transformed and cultured per the manufacturer's instructions, and ampicillin-resistant isolates were screened by PCR using vector- and insert-specific primers. Plasmids derived from positively scoring transformants were extracted using the QIAprep Spin Miniprep Kit (QIAGEN; #27106) and validated by Sanger sequencing (Quintarabio; www.quintarabio.com/).

Minimal backbone segments, containing solely the bacterial replication origin, ampicillin marker, yeast replication origin, and yeast selection marker, were sourced from the p415 and p426 expression series developed by Mumberg *et al.* (*56*). For strong transcription in yeast coupled to glycolytic activity, we either retained the *TDH3* ("GPD") or *TEF1* promoters from the Mumberg vectors or cloned the −703 to −1 fragment of the *PDC1* promoter from FY4/5 genomic DNA. Protein coding sequences for *ADH6*, *ADH7*, and *GRE2* were likewise amplified directly from FY4/5 genomic DNA. For *ADH4* from *S. stipitis*, we contracted with Bio Basic (www.biobasic.com) to synthesize a *S. cerevisiae* codon-optimized sequence from the publicly available protein translation (GenBank accession no. XM_001387085). Similarly, *ldhA* from *L. mesenteroides* subsp. *mesenteroides* was produced by Eurofins Genomics (www.eurofinsgenomics.com) from the amino acid sequence available from UniProt (gene entry LEUM_1756). For transcription termination, we either retained the *CYC1* element from Mumberg or, from FY4/5 genomic DNA, cloned the 166 bp immediately following the stop codon of *ADH1* or the 295 bp following *ACT1*.

To clone the *GRE2* mutants emerging from toxicity selection, the plasmid-based coding sequences were distinguished from chromosomal *GRE2* via an initial PCR using primers binding to library plasmid elements. Specifically, the collection of mutagenized genes, including their nonmutagenized promoters and terminators, was originally subcloned via Gateway recombination and positioned between attB1 and attB2 sequences (*36*). Thus, from total DNA isolated from the final inhibitor-tolerant culture (fig. S4), we performed an initial amplification using primers annealing to these unique attB elements. To further subclone the coding sequences of hypertolerant *GRE2* mutants, the plasmid-derived amplicons were used to template a second-pass PCR excluding the *GRE2* promoter and terminator. These amplified protein-coding fragments were subsequently Gibson-assembled into our final expression constructs. See table S4 for a complete list of overexpression plasmids used in this study.

Yeast strain construction

Recombinant strains were created following the lithium acetate chemical transformation method of Gietz *et al.* (*57*). For single plasmid introduction, 50 ng of p(RS)415-based DNA was used with one OD_{600} unit of cells and selection carried out on solid YSC-Leu dropout medium. For strains originating from two simultaneous plasmids, 150 to 300 ng each of p426TEF- and p(RS)415-based DNA was used with three to four OD_{600} units, and selection was performed on YSC-Ura-Leu solid medium. For chromosomal integrations, 800 ng to 1 μg of linear DNA was used with 7 to 10 OD_{600} units. Low transformation efficiencies (e.g., from variability in strain, locus, and DNA secondary structure) were typically resolved by increasing the DNA to cell ratio, amount of salmon sperm carrier DNA, or heat shock incubation time (up to 40 to 50 min at 42°C). In addition to laboratory standard BY4743, the *gre2*Δ::kanMX4/*gre2*Δ::kanMX4 diploid used for LAMy629 preexisted this study and was obtained from the *Saccharomyces* Genome Deletion Project collection (www-sequence.stanford.edu/group/yeast_deletion_project/).

To create the diploid xylose-consuming chassis (XYL^+), a xylose-enabled *MAT*a *leu2-3* haploid (internal strain F258) available from the development efforts of Zhou *et al.* (*46*) was transformed with plasmid pJH727 (*GAL::HO LEU2*; gift from J. Haber of Brandeis University) to generate a *MAT*α equivalent (*46*, *58*). Induction of *HO* in Leu^+ transformants was conducted in liquid medium containing 20 g/liter of galactose for 6 hours at 30°C (complete mating type switching protocol, including preinduction, is available from the Haber Lab website: www.bio.brandeis.edu/haberlab/jehsite/protocol.html). Individual colonies, recovered from growth in glucose medium additionally containing leucine to discard pJH727, were screened for *MAT*α haploids by α- and a-factor sensitive mating type tester strains (*59*). A validated *MAT*α *leu2-3* haploid was subsequently mated with F258 to create the homozygous XYL^+ leu^- chassis strain LAMy435 that preceded LAMy419 and LAMy665.

To create the S288C leu^- predecessor of LAMy660, LAMy661, and LAMy663, the defective *his3Δ1* and *ura3Δ0* alleles in BY4743 were complemented sequentially by targeted chromosomal replacements. Briefly, a PCR product encompassing the full-length coding sequence of *HIS3* was amplified from FY4/5 genomic DNA, introduced into BY4743, and transformants selected for histidine prototrophy. To repair *ura3Δ0*, which spans a segment larger than the open reading frame of *URA3*, a PCR product including 320 bp of the *URA3* promoter and 194 bp beyond the stop codon was amplified from FY4/5 genomic DNA, introduced into the His^+ intermediate, and transformants selected on minimal YNB medium supplemented solely with leucine to yield chassis strain LAMy651.

To create the diploid ethanol-handicapped chassis for lactic acid production, we first generated a fully ethanol-deficient pdc^- haploid by creating a markerless deletion of *PDC5* in a *MAT*a *pdc1*Δ::kanMX4 strain sourced from the *Saccharomyces* Genome Deletion Project collection (*PDC6*, while intact, is functionally inert). Briefly, plasmid pCRSPR,PDC1+5 expressing a *Candida albicans*/*S. cerevisiae* codon-optimized version of Cas9, as well as a guide RNA targeting the protospacer adjacent motif (PAM)–proximal sequence TGCTAAGAACCCAGTTATCT common to *PDC1* and *PDC5*, was coelectroporated with the double-stranded linear repair template CATAATCAATCTCAAAGAGAACAACACAATACAATAACAAGAAGAACAAAGCTAATTAAC into the *MAT*a *pdc1*Δ::kanMX4 haploid according to the protocol of Vyas *et al.* (*60*) (plasmid and template are gifts of B. Uranukul). Transformants were selected on solid YP (yeast bacto-peptone) medium containing 3% ethanol, 3% glycerol, and nourseothricin (YPEG + NAT) (100 μg/ml), and isolates comparatively grown on YPEG + NAT and YPD (YP with 2% glucose) solid media to identify the pdc^- phenotype (development strain LAMy399).

Separately, a haploid containing *PDC5* transcribed by the low-strength *TEF1*m4 promoter mutant was generated in a *MAT*α *pdc1*Δ::kanMX4 strain sourced from the *Saccharomyces* Genome Deletion Project collection. Here, the in-locus markerless edit was likewise accomplished through a similar CRISPR protocol with plasmid LAMb66 (featuring uracil selection in yeast and improved Cas9 expression) encoding a guide RNA targeting sequence TTCTCGATCAATATACTGTA in the *PDC5* promoter and the double-stranded

repair template CAAAGGTCGCGTTTCTTTTAGAAAAACTA-ATACGTAAACCTGCATTAAGGGAACAAAAGCTGGAGCT-CATAGCTTCAAAAcGcTTCTACcCCcTTTTTACTCTTC-CAGATTTTCTCGGACTCCGCGCATCGCCGTACCACTTCAA-g A C A C C C A A G C A C A G C A T A C T A A A T T T C -CCCTCTTTCTTCCTCTAGGGTGTCGcTAATTACCCG-TACTAAAGGTTTGGAAAAGAAAAAAGgGACCGCCTC-GTTTCTTTcTCTTCGTCGAgAgAGGCAATAAAAATTTTTAT-C A C G T T T C T T T T T C T T G A g A g T T T c T T T c T t -GATTTTTTTCTCTTTCGATGACCTCCCATTGATATTTA-A G c T A A T A A A C G G T C T T C A A T T T C T -C A A G c T T C A G T T T C A T T T T T C T T G T T C T A T T A -CAACTTTTTTTACTTCTTGCTCgTTAGAgAGAAAG-CATAGCAATCTAATCTAAGTTTTCTAGAAAAATGTCT-GAAATAACCTTAGGTAAATATTTATTTGAAAGATTGAGC-CAAGT where lowercase letters designate the *TEF1*m4 promoter mutations (*50*). Transformants were selected on YSC-Ura solid medium, and small colonies suggesting handicapped glucose growth were validated further by PCR using primer pairs identifying the *TEF1*m4 promoted-*PDC5* fusion. This haploid was mated to LAMy399 to produce the *PDC5* heterozygote, and the diploid subsequently made His^+ via the chromosomal integration described above to yield the ethanol-handicapped chassis strain LAMy670 preceding LAMy690 and LAMy692.

All final strains were revalidated by PCR using plasmid- or modification-specific primers and the relevant regions Sanger sequenced as appropriate before fermentation experiments. See table S5 for a complete list of strains used in this study.

Media and fermentation conditions

To provide a consistent but modifiable medium to accommodate our entire collection of strains, all baseline culturing was performed in YSC composed of 1.5 g/liter of YNB without amino acids and ammonium sulfate (BD Difco, #233520; www.bd.com), 5 g/liter of ammonium sulfate, 0.2 mM inositol, 0.1 g/liter of each of the 20 amino acids, and 0.1 g/liter each of adenine and uracil (all from Sigma-Aldrich; www.sigmaaldrich.com). Strains containing a p(RS)415 plasmid were maintained in medium lacking leucine and those with a p426 plasmid lacking uracil. Unless indicated otherwise, individual strains were expanded and acclimated to high cell density and high sugar conditions in singlicate YSC-based cultures and divided into triplicate biological samples upon inoculation into fermentation (Fig. 1, A to C, 2, and 3) or growth (Fig. 1D) media. All yeast culturing and fermentations were conducted at 30°C in Erlenmeyer flasks (≥25 ml) shaken at 200 rpm or glass tubes (≤12 ml) rotated in a cell culture roller drum at maximum speed.

For the constituent toxicity studies, prototrophic strain FY4/5 was expanded in a starter culture of YSC containing 150 g/liter of glucose and grown overnight to approximately OD_{600} = 10. To mimic industrial high cell density conditions, 100 OD_{600} units of cells per fermentation were harvested and washed with an equal volume of room-temperature distilled and deionized water, and cell pellets were resuspended in 4 ml of media for a production cell density of approximately OD_{600} = 25 (9.9 g of dry cell weight/liter). Fermentation media contained 250 g/liter of glucose in YSC and were supplemented with (left to right in Fig. 1A) 6 mM NH_4Cl, 50/6 mM KCl/NH_4OH, 100/128 mM acetic acid/NH_4Cl, 100/50/128 mM acetic acid/KCl/NH_4Cl, 100/50/128 mM acetic acid/KCl/NH_4OH, 100/11 mM furfural/NH_4Cl, 100/50/11 mM furfural/KCl/NH_4OH, 100/7 mM FF-OH/NH_4Cl, 100/50/7 mM FF-OH/KCl/NH_4Cl, 100/50/7 mM FF-OH/KCl/NH_4OH, 100/7 mM HMF/NH_4Cl, 100/50/7 mM HMF/KCl/NH_4OH, 100/7 mM HMF-OH/NH_4Cl, 100/50/7 mM HMF-OH/KCl/NH_4Cl, or 100/50/7 mM HMF-OH/KCl/NH_4OH. Inhibitor supplementations for the additionally screened conditions in fig. S1 were 50/60 mM acetic acid/NH_4Cl, 50/50/60 mM acetic acid/KCl/NH_4OH, 150/180 mM acetic acid/NH_4Cl, 150/50/180 mM acetic acid/KCl/NH_4OH, 50/9 mM furfural/NH_4Cl, 50/50/9 mM furfural/KCl/NH_4OH, 50/6 mM FF-OH/NH_4Cl, 50/50/6 mM FF-OH/KCl/NH_4OH, 150/15 mM furfural/NH_4Cl, 150/50/15 mM furfural/KCl/NH_4OH, 150/9 mM FF-OH/NH_4Cl, 150/50/9 mM FF-OH/KCl/NH_4OH, 50/6 mM HMF/NH_4Cl, 50/50/6 mM HMF/KCl/NH_4OH, 50/6 mM HMF-OH/NH_4Cl, 50/50/6 mM HMF-OH/KCl/NH_4OH, 150/11 mM HMF/NH_4Cl, 150/50/11 mM HMF/KCl/NH_4OH, 150/9 mM HMF-OH/NH_4Cl, or 150/50/9 mM HMF-OH/KCl/NH_4OH. The "/" notation is used for visual abbreviation but indicates the addition of all components during preparation. All NH_4OH concentrations were predetermined to be the amounts needed to achieve pH 6; the same concentration of NH_4Cl was supplemented to the inhibitor-only condition to control for ammonium addition (that said, our prior experience has shown that yeast can tolerate at least 200 mM NH_4Cl with no detectable changes on ethanol titer). Furfural (Sigma-Aldrich, #185914), HMF (Sigma-Aldrich, #H40807), FF-OH (Sigma-Aldrich, #W249106), and HMF-OH (Santa Cruz Biotechnology, #sc-210242; www.scbt.com) were added directly to media in their supplier, concentrated form to minimize the addition of volume. Despite the highly nonpolar nature of furfural and HMF, substantial agitation during media preparation was sufficient to solubilize these components such that amounts added and those quantified from high-performance liquid chromatography (HPLC) were in agreement. Fermentation samples of 550 µl were harvested after 48 hours, cells were removed by centrifugation (16,870*g*, 2 min), and supernatants were 0.45-µm syringe-filtered (Thermo Fisher Scientific, #50-109-8735; www.fishersci.com) into glass HPLC vials and stored at 4°C until analysis. Similarly, preinoculation fermentation media were syringe-filtered and diluted 5^{-1} in water for HPLC verification of starting glucose and inhibitor concentrations.

To screen the panel of overexpressed reductases on fermentation (fig. S2), strains LAMy312, LAMy553, LAMy579, LAMy580, and LAMy589 were started in YSC-Leu containing 180 g/liter of glucose and diluted for further acclimation overnight to higher glucose in YSC-Leu containing 240 g/liter of glucose. Upon reaching OD_{600} = 2.5 to 3, 100 OD_{600} units of cells were harvested, and cell pellets were resuspended in 4 ml of YSC-Leu containing 260 g/liter of glucose, 62/48/100 mM furfural/HMF/acetic acid, and 60/140 mM $KHCO_3$/$CaCO_3$. A second set of cell pellets was resuspended in 4 ml of YSC-Leu containing 240 g/liter of glucose, 84/64/133 mM furfural/HMF/acetic acid, and 60/200 mM $KHCO_3$/$CaCO_3$. Cell-free samples of the fermentation medium were harvested after 46 hours per procedure described above for HPLC analysis.

To prepare samples for mass spectrometric quantification of furfural, HMF, FF-OH, and HMF-OH (Fig. 1B), strains LAMy312 and LAMy579 were started in YSC-Leu containing 180 g/liter of glucose and diluted for further acclimation overnight to higher glucose in YSC-Leu containing 240 g/liter of glucose. Upon reaching OD_{600} = 2.5 to 3, 100 OD_{600} units of cells were harvested, and cell pellets were resuspended in 4 ml of YSC-Leu containing 260 g/liter of glucose, 62/48/100 mM furfural/HMF/acetic acid, and 60/140 mM $KHCO_3$/$CaCO_3$. After 24 hours of fermentation, 100 µl of supernatant from cell-pelleted

samples was combined with 100 µl of 100% ultra-HPLC (UHPLC)–grade methanol containing isotopically labeled amino acids (provided by the Whitehead Institute Metabolite Profiling Core Facility), and mixtures were stored at −80°C until analysis. Similarly, 100 µl of syringe-filtered preinoculation fermentation medium was extracted to determine starting concentrations of inhibitors.

To assess the impact of *GRE2* and increasing K^+ and pH conditions on cell viability under combined furan aldehyde stress (Fig. 1C and fig. S3), strains LAMy312, LAMy579, and LAMy629 were started in YSC-Leu containing 180 g/liter of glucose, diluted, and further acclimated overnight in YSC-Leu containing 260 g/liter of glucose. Upon reaching OD_{600} = 2.5 to 3, 100 OD_{600} units of cells were harvested, and cell pellets were resuspended in 4 ml of YSC-Leu containing 260 g/liter of glucose, 62/48 mM furfural/HMF, and supplemented with (from blue to red) 25 mM KCl, 5 mM NH_4OH, 10 mM NH_4OH, 15 mM NH_4OH, 20 mM NH_4OH, 24 mM NH_4OH, 24/25 mM NH_4OH/KCl, 24 + 5 mM NH_4OH + NH_4OH, 24 + 10 mM NH_4OH + NH_4OH, 24 + 15 mM NH_4OH + NH_4OH, or 24 + 20 mM NH_4OH + NH_4OH. As above, "/" indicates addition of components during preparation, while the "+" here indicates addition after 22 hours of fermentation. At 0, 24, 32, 52, and 71 hours after inoculation, cell densities were measured, and 20 µl was taken for immediate methylene blue viability staining and microscopy (fig. S3). Preinoculation media and cell-free fermentation samples at 71 hours were harvested for HPLC analysis.

To screen for a fermentation advantage conferred by overexpression of $GRE2^{evol}$ versus *GRE2* (fig. S5A), prototrophic strains LAMy660, LAMy661, and LAMy663 were started in minimal YNB medium (i.e., no amino acids) containing 100 g/liter of glucose and diluted for further acclimation overnight to higher glucose in 1.3× YNB containing 240 g/liter of glucose. Upon reaching OD_{600} = 2.5 to 3, 100 OD_{600} units of cells were harvested, and cell pellets were resuspended in 4 ml of YSC-Leu containing 260 g/liter of glucose, 62/48/100 mM furfural/HMF/acetic acid, and 60/140 mM $KHCO_3$/$CaCO_3$. A second set of cell pellets was resuspended in 4 ml of YSC-Leu containing 280 g/liter of glucose, 62/48/100 mM furfural/HMF/acetic acid, and 60/140 mM $KHCO_3$/$CaCO_3$. A third set of cell pellets was resuspended in 4 ml of YSC-Leu containing 260 g/liter of glucose, 84/63/100 mM furfural/HMF/acetic acid, and 60/140 mM $KHCO_3$/$CaCO_3$. For fig. S5B, LAMy660 and LAMy663 prepared and harvested in the same fashion were resuspended in 4 ml of YNB containing 260 g/liter of glucose, 62/48/100 mM furfural/HMF/acetic acid, and 60/200 mM KCl/$CaCO_3$. Here, because of the reduced acidity from the lack of amino acids in YNB, equimolar KCl was used in lieu of $KHCO_3$, and $CaCO_3$ consequently increased to 200 mM, to achieve a pH within range of that in equivalent YSC-Leu. For fig. S5C, LAMy660, LAMy663, LAMy690, and LAMy692 were started in YSC–Ura-Leu-His-Trp-Ade-Lys ("YSC–6 AA") dropout medium containing 100 g/liter of glucose, diluted, and further expanded overnight in YSC–6 AA containing 250 g/liter of glucose (LAMy660 and LAMy663) or 150 g/liter of glucose (LAMy690 and LAMy692). Upon reaching OD_{600} = 2.5 to 3, 100 OD_{600} units of LAMy660, 663 were harvested, and cell pellets were resuspended in 4 ml of YSC-Leu with 260 g/liter of glucose and 60/140 mM $KHCO_3$/$CaCO_3$. For LAMy690 and LAMy692, 90 OD_{600} units were harvested and resuspended in 4 ml of YSC-Ura-Leu with 165 g/liter of glucose and 60/250 mM $KHCO_3$/$CaCO_3$. Cell-free samples of the fermentation medium were harvested after 40 hours (fig. S5A), 48 hours (fig. S5B), or 24 hours (fig. S5C) for HPLC analysis.

For assaying a fitness advantage conferred by $GRE2^{evol}$ versus *GRE2* overexpression (Fig. 1D), strains LAMy660, LAMy661, and LAMy663 were started in YSC–6 AA medium containing 100 g/liter of glucose, diluted, and further expanded overnight in YSC–6 AA containing 250 g/liter of glucose. Upon reaching OD_{600} = 2.5 to 3, nine OD_{600} units of cells were harvested, and cell pellets were resuspended in 13.5 ml of YSC–6 AA containing 50 g/liter of glucose, 40/28/55 mM furfural/HMF/acetic acid, supplemented with 50 mM KCl, and adjusted to pH 6 with NH_4OH. Cell densities were measured at 0, 24, 48.5, 51.5, 56, 65.5, 69, 72, 75.5, 79.5, 91, and 96.5 hours after inoculation. Cell-free samples of the medium were collected at 0, 24, 48.5, 56, 65.5, 72, 79.5, and 96.5 hours for determination of furfural and HMF concentrations by HPLC.

For the fermentation time courses of Fig. 2A, strains LAMy660 and LAMy663 were started in YSC–6 AA containing 100 g/liter of glucose, diluted, and further expanded overnight in YSC–6 AA containing 250 g/liter of glucose. Upon reaching OD_{600} = 2.5 to 3, 100 OD_{600} units of LAMy660 were harvested, and cell pellets were resuspended in 4 ml of YSC-Leu with 260 g/liter of glucose and 60 or 140 mM $KHCO_3$/$CaCO_3$ (uninhibited control, blue), 62/48/100 mM furfural/HMF/acetic acid and adjusted to pH 5 with NH_4OH per bioethanol practices (inhibited control, red), or 62/48/100 mM furfural/HMF/acetic acid and 60/140 mM $KHCO_3$/$CaCO_3$ (orange). This final condition, as well as that of the inhibited control (inhibitor trio adjusted to pH 5 with NH_4OH), was repeated with 100 OD_{600} units of strain LAMy663 for direct comparison with LAMy660 (gray solid and gray dotted, respectively). At 0, 16, 32, and 48 hours after inoculation, cell-free samples of the fermentation medium were harvested for HPLC analysis.

To assess performance in genuine biomass feedstocks (Fig. 2B), strains LAMy660 and LAMy663 were started in YSC-Leu containing 100 g/liter of glucose, diluted, and further expanded overnight in YSC-Leu containing 250 g/liter of glucose. Upon reaching OD_{600} = 2.5 to 3, 90 OD_{600} units were harvested, and cell pellets were resuspended in 4 ml of the seven indicated lignocellulosic hydrolysates supplemented with 20 mM urea and modified as follows: In the minimally altered control (blue), $Ca(OH)_2$ was also added, if necessary, to achieve pH 5; in the inhibited control (red), feedstocks were toxified to the final concentrations of glucose, furfural, HMF, and acetic acid listed in table S2 (white columns) and adjusted to pH 5 with $Ca(OH)_2$ if needed; and in the toxification and K^+/pH-ameliorated condition (orange), feedstocks were toxified identically but adjusted instead with $KHCO_3$, $CaCO_3$, and $Ca(OH)_2$ as listed in table S2 (white and gray columns). These three conditions were fermented with LAMy660, and the final was repeated with LAMy663 (gray). The ordering and color scheme of bars in Fig. 2B follow that of Fig. 2A. The "high concentration sugar syrup" nature of DMR corn stover as described by the provider was found in pilot experiments to be inhibitory to yeast (above-average concentrations of glucose and xylose were confirmed; see table S1); therefore, dilutions of 65 to 75% were necessary to enable fermentation (*61*). All supplements were added in the maximally concentrated forms available to minimize dilution of the original hydrolysate. The minimally altered controls (blue) for bagasse, wheat straw, miscanthus, and switchgrass hydrolysate were observed in preliminary experiments to be sufficiently low in available sugar and ethanol product inhibition such that ethanol was metabolized following the consumption of glucose. To maximize accuracy of titers, cell-free fermentation samples for HPLC analysis were harvested after 24 hours under these four control conditions and 52 hours in all remaining.

For demonstrating extensibility of hydrolysate tolerance to xylose-consuming strains (Fig. 3A), prototrophic strains LAMy419 and LAMy665 were started in YSC–6 AA containing 40 g/liter of xylose, diluted, and further expanded overnight in YSC–6 AA containing 100 g/liter of xylose. Upon reaching OD_{600} = 2.5 to 3, 90 OD_{600} units were harvested, and cell pellets were resuspended in 4 ml of bagasse, high-acid corn stover, or miscanthus hydrolysate (nonbold) supplemented with 20 mM urea and modified in the same order and manner as those described above for Fig. 2B: Blue contained the $Ca(OH)_2$ needed to achieve pH 5 and was fermented with LAMy419; red toxified to the conditions listed in table S2 (white columns) and fermented with LAMy419; orange was toxified, K^+ and pH-adjusted to the conditions in table S2 (white and gray columns) and fermented with LAMy419; and gray was the same as orange but fermented with LAMy665.

Formulation and fermentation of synthetic medium (bold) was performed in a manner to reflect genuine lignocellulosic hexose-pentose proportions but maintain the xylose metabolism that would be suppressed from catabolite repression. Specifically, LAMy419 was fermented in YSC–6 AA prepared with 50 g/liter of xylose, 150 g/liter of potato starch (Sigma-Aldrich, #S2630), and 60/140 mM $KHCO_3/CaCO_3$ (uninhibited control, blue), 62/48/100 mM furfural/HMF/acetic acid and adjusted to pH 5 with NH_4OH (inhibited control, red), or 62/48/100 mM furfural/HMF/acetic acid and 60/140 mM $KHCO_3/CaCO_3$ (orange). The final condition was repeated with LAMy665 (gray). For these four conditions, the harvested 90 OD_{600} units were resuspended in 2.5 ml of medium and glucoamylase (Sigma-Aldrich, #A7095) added in the following amounts and times: 333 μl at 0 hour (+25 U/ml), 333 μl at 18 hours, 666 μl at 24 hours (+50 U/ml), and 666 μl at 36.5 hours. Enzyme amounts and times of addition were predetermined in pilot experiments to support the full consumption of xylose in the uninhibited control (see also fig. S8). Fermentation media were prepared in the most concentrated form possible to minimize dilution from glucoamylase addition. Cell-free fermentation samples for HPLC analysis were harvested after 48 hours for the uninhibited controls (blue) to minimize ethanol loss to consumption and 72 hours for the remaining conditions.

For demonstrating extensibility of hydrolysate tolerance to lactic acid–producing strains (Fig. 3B), prototrophic strains LAMy690 and LAMy692 were started in YSC–6 AA containing 100 g/liter of glucose, diluted, and further expanded overnight in YSC–6 AA containing 200 g/liter of glucose. Upon reaching OD_{600} = 2.5 to 3, 90 OD_{600} units of LAMy690 were harvested, and cell pellets were resuspended in 4 ml of YSC–Ura-Leu (bold) with 160 g/liter of glucose and 60/250 mM $KHCO_3/CaCO_3$ (uninhibited control, blue), 62/48/100 mM furfural/HMF/acetic acid and adjusted to pH 5 with NH_4OH (inhibited control, red), or 62/48/100 mM furfural/HMF/acetic acid and 60/270 mM $KHCO_3/CaCO_3$ (orange). The final condition was repeated with LAMy692 (gray). Cell-free fermentation samples for HPLC analysis were harvested after 24 hours for the uninhibited control (observed in pilot experiments to have had all glucose consumed) and 72 hours for toxified conditions. For production from genuine hydrolysates, 90 OD_{600} units of LAMy690 (blue, red, and orange conditions) or LAMy692 (gray) were resuspended in 4 ml of 65% DMR corn stover, low-acid corn stover, or wheat straw hydrolysate (nonbold) supplemented with 20 mM urea and modified largely in the same order and manner as those described for Fig. 3A: Blue additionally contained 280, 200, or 120 mM $CaCO_3$, respectively, to buffer lactic acid accumulation; red toxified to the conditions listed in table S2 (white columns); and orange and gray were toxified, K^+ and pH-buffered to the conditions in table S2 (white and gray columns). Cell-free fermentation samples for HPLC analysis were harvested after 24 hours (wheat straw, blue) or 48 hours (DMR and low-acid corn stover, blue) for the uninhibited controls (observed in pilot experiments to have had all glucose consumed) and after 72 hours for toxified conditions.

Directed evolution of *GRE2*

We revived the PCR-mutagenized *GRE2* yeast library from the "functional variomics" collection (gift of X. Pan of Baylor University) in YSC-Ura containing 30 g/liter of glucose and supplemented with 10 mM KH_2PO_4 (*36*). To maintain the $>2 \times 10^5$ diversity, 20 μl of thawed cells were expanded to saturation, diluted, and cultured overnight in fresh medium to approximately OD_{600} = 2.5. Cell biomass totaling 3.5 OD_{600} units was harvested and resuspended in 4 ml of YSC-Ura containing 30 g/liter of glucose, 32/25/52 mM furfural/HMF/acetic acid, supplemented with 10 mM KH_2PO_4, and adjusted to pH 6 with NH_4OH. Following the time course of fig. S4, cell densities reaching OD_{600} values of 5 to 8 were subcultured in identically formulated YSC-Ura medium containing the indicated combinations of inhibitors. A 1-ml aliquot of the final culture was harvested for isolation of bulk DNA and the remaining mixed to 15% glycerol for preservation at −80°C.

Several attempts were required to converge on the conditions used in the successful iteration depicted in fig. S4. For example, the 62/48/100 mM furfural/HMF/acetic acid combination used as our fermentation benchmark was determined to be growth suppressive even when pH-adjusted to neutralize acetic acid. A reduction to 30/24/50 mM furfural/HMF/acetic acid provided baseline growth-permissive conditions; however, increments of 5 to 10% of each inhibitor at the first subculturing ended in suppression. Given these responses, we hypothesized that prolonging stress combinations over multiple expansion cycles was needed to allow stronger mutants to entrench within the population and seed further advantageous trajectories. Last, that the hypertolerant $GRE2^{evol}$ mutant was capable of conferring an improvement to fermentation under the benchmark suite of inhibitors (Fig. 2A), yet still unable to demonstrate growth under the same conditions (fig. S9), underscored the divergence in tolerance thresholds between metabolic and biomass production.

The coding sequence for the $GRE2^{evol}$ allele is as follows: ATGTCAGTTTTCGTTTCAGGTGCTAACGGGTTCATTGCCCAACACATTGTCGATCTCCTGTTGAAGGAAGACTATAAGGTCATCGGTTCTGCCAGAAGTCAAGAAAAGGCCGAGAATTTAACGGAGGCCTTTGGTAACAACTCAAAATTCTCCATGGAAGTTGTCCCAGACATATCTAAGCTGGACGCATTTGACCATGTTTTCCAAAAGCACGGCAAGGATATCAAGATAGTTCTACATACGGCCTCTCCATTCTGCTTTGATATCACTGACAGTGAACGCGATTTATTAATTCCTGCTGTGAACGGTGTTAAGGGAATTCTCCACTCAATTAAAAAATACGCCGCTGATTCTGTAGAACGTGTAGTTCTCACCTCTTCTTATGCAGCTGTGTTCGACATGGCAAAAGAAAACGATAAGTCTTTAACATTTAACGAAGAATCCTGGAACCCAGCTACCTGGGAGAGTTGCCAAAGTGACCCAGTTAACGCCTACTGTGGTTCTAAGAAGTTTGCTGAAAAAGCAGCTTGGGAATTTCTAGAGGAGAATAGAGACTCTGTAAAATTCGAATTAACTGCCGT

TAACCCAGTTTACGTTTTTGGTCCGCAAATGTTTGA-CAAAGATGTGAAAAAACACTTGAACACATCTTGC-GAACTCGTCAACAGCTTGATGCATTTATCACCAGAGGA-CAAGATACCGGAACTATTTGGTGGATACATTGATGTTC-GTGATGTTGCAAAGGCTCATTTAGTTGCCTTCCAAAA-GAGGGAAACAATTGGTCAAAGACTAATCGTATCGGAGG-CCAGATTTACTATGCAGGATGTTCTCGATATCCTTAAC-GAAGACTTCCCTGTTCTAAAAGGCAATGTTCCAGTGGG-GAAACCAGGTTCTGGTGCTACCCATAACACCCTTGGTGC-TACTCTTGATAATAAAAAGAGTAAGAAATTGTTAG-GTTTCAAGTTCAGGAACTTGAAAGAGACCATTGACGA-CACTGCCTCCCAAATTTTAAAATTTGAGGG-CAGAATATAA.

Chromatography

Quantification of ethanol, lactic acid, glucose, xylose, glycerol, furfural, HMF, and acetic acid was performed on cell-free, 0.45-μm filtered samples using an Agilent 1200 Infinity Series HPLC configured with G1362A Refractive Index Detector and Aminex HPX-87H carbohydrate analysis column (Bio-Rad, #125-0140; www.bio-rad.com). Analytes were separated isocratically in 5 mM sulfuric acid at 65°C using a flow rate of 0.6 m/min. Under these conditions, retention times were approximately as follows: glucose, 9.2 min; xylose, 9.9 min; lactic acid, 13.1 min; glycerol, 13.8 min; acetic acid, 15.3 min; ethanol, 22.3 min; HMF, 30.2 min; furfural, 45.0 min. Chromatogram peaks autointegrated by the Agilent OpenLab CDS ChemStation software were converted to concentrations through interpolation off standard curves calibrated over the ranges of 0 to 100 g/liter of glucose, 0 to 50 g/liter of xylose, 0 to 100 g/liter of lactic acid, 0 to 8 g/liter of glycerol, 0 to 60 g/liter of acetic acid, 0 to 150 g/liter of ethanol, 0 to 8 g/liter of HMF, and 0 to 8 g/liter of furfural defined from chemically pure dilution series. To compensate for the minor overlap between the peaks for glucose and xylose, we used standards incorporating the two sugars at a ratio of 3:1 g/liter of glucose:xylose to reflect typical proportions. Likewise, lactic acid and glycerol standards incorporated 10:1 g/liter of lactic acid:glycerol.

Given the likelihood of calcium salts precipitating from the low pH in the running solvent and obstructing instrument fluidic lines, all samples derived from calcium-containing fermentations were acidified with 1% sulfuric acid (vol/vol), rotated for ≥1 hour at 4°C, precipitates removed via centrifugation, and supernatants 0.45-μm filtered before HPLC analysis.

Mass spectrometry

For targeted quantification of furfural, FF-OH, HMF, and HMF-OH, cell-free samples collected from fermentation were extracted 1:1 with 100% UHPLC-grade methanol containing seventeen ^{13}C labeled amino acids (Cambridge Isotope Laboratories; www.isotope.com) added as internal standards and stored at −80°C for further processing. Amino acid–methanol extraction buffer, downstream method development, and analysis were provided by the Metabolite Profiling Core Facility at the Whitehead Institute (metabolomics.wi.mit.edu).

In brief, additional dilutions to 20^{-1} and 80^{-1} (final) in 50% methanol were required to reach the linear range of the spectrometer. Samples of 1 μl were injected into a Dionex UltiMate 3000 ultra-high performance liquid chromatography (UPLC) unit equipped with an Ascentis Express C18 (2.1 mm by 150 mm, 2.7 μm particle size) column (Sigma-Aldrich, #53825-U) maintained at 35°C. Analytes were reverse phase separated at a flow rate of 0.25 ml/min using buffers A [0.1% formic acid in liquid chromatography–mass spectrometry (LC–MS) grade water] and B (0.1% formic acid in LCMS grade acetonitrile) under the following gradient conditions: 0 to 2 min (5% B); 2 to 20 min (5 to 75% B, linear gradient); 20.1 to 24 min (95% B); 24.1 to 28 min (5% B). Mass analysis was performed on a Thermo Fisher Scientific Q Exactive Orbitrap operating with a spray voltage of 3.0 kV, capillary temperature 275°C, HESI probe temperature 350°C, sheath gas flow 40 units, auxiliary gas flow 15 units, and sweep gas flow 1 unit. For targeted isolation of furfural, HMF, FF-OH, and HMF-OH, positive ionization mode was used with resolution set to 70,000, automatic gain control to 1×10^5 with maximum injection time of 250 ms, and isolation window to 4.0 m/z. Fragmentation patterns from MS/MS were matched with reference spectra available in the METLIN online database (metlin.scripps.edu). Quantification was performed using the Thermo Fisher Scientific Xcalibur Software calibrated against chemically pure dilution series of 3 μM to 3 mM furfural, 30 μM to 3 mM FF-OH, 0.1 μM to 3 mM HMF, and 30 μM to 3 mM HMF-OH.

For measurement of salt concentrations in hydrolysates, 10 ml of each sample was centrifuged (3500*g* for 5 min) to remove large particulates, and the supernatants submitted to Environmental Testing and Research Laboratories (etrlabs.com) for quantification of K^+ and Ca^{2+} (available as components of their water testing suite). Acid-digested samples were assayed in three replicate reads by inductively coupled plasma mass spectrometry.

Viability measurements

Yeast population viabilities measured via methylene blue staining and subsequent procedures to calculate correlation with ethanol titers were described previously (*16*).

Statistical analysis

Calculation of SD, propagation of error, hypothesis testing (two-sample, two-tailed *t* test, $\alpha = 0.05$), and *P* value determination were performed using MATLAB (The MathWorks; www.mathworks.com) on independent biological triplicates following standard procedures.

SUPPLEMENTARY MATERIALS

Supplementary material for this article is available at http://advances.sciencemag.org/cgi/content/full/7/26/eabf7613/DC1

View/request a protocol for this paper from *Bio-protocol*.

REFERENCES AND NOTES

1. C. McKerracher, A. Izadi-Najafabadi, A. O'Donovan, N. Albanese, N. Soulopoulous, D. Doherty, M. Boers, R. Fisher, C. Cantor, J. Frith, S. Mi, A. Grant, "Electric vehicle outlook 2020" (Bloomberg New Energy Finance, Bloomberg Finance L.P., 2020).
2. S. Davis, R. G. Boundy, *Transportation Energy Data Book: Edition 38* (ORNL/TM-2019/1333, Oak Ridge National Laboratory, 2020).
3. Y. M. Bar-On, R. Phillips, R. Milo, The biomass distribution on Earth. *Proc. Natl. Acad. Sci. U.S.A.* **115**, 6506–6511 (2018).
4. M. H. Langholtz, B. J. Stokes, L. M. Eaton, *2016 Billion-Ton Report: Advancing Domestic Resources for a Thriving Bioeconomy* (2016); http://energy.gov/eere/bioenergy/2016-billion-ton-report.
5. W.-C. Wang, L. Tao, J. Markham, Y. Zhang, E. Tan, L. Batan, E. Warner, M. Biddy, "Review of biojet fuel conversion technologies" (Technical Report NREL/TP-5100-66291, 1278318, 2016).
6. N. W. Y. Ho, M. R. Ladisch, M. Sedlak, N. S. Mosier, E. Casey, Biofuels from cellulosic feedstocks, in *Comprehensive Biotechnology (Second Edition)*, M. Moo-Young, Ed. (Elsevier B.V., 2011), vol. 3, pp. 51–62.
7. L. J. Jönsson, B. Alriksson, N. O. Nilvebrant, Bioconversion of lignocellulose: Inhibitors and detoxification. *Biotechnol. Biofuels* **6**, 16 (2013).

8. E. C. van der Pol, R. R. Bakker, P. Baets, G. Eggink, By-products resulting from lignocellulose pretreatment and their inhibitory effect on fermentations for (bio) chemicals and fuels. *Appl. Microbiol. Biotechnol.* **98**, 9579–9593 (2014).
9. L. R. Lynd, The grand challenge of cellulosic biofuels. *Nat. Biotechnol.* **35**, 912–915 (2017).
10. N. Ali, Q. Zhang, Z.-Y. Liu, F.-L. Li, M. Lu, X.-C. Fang, Emerging technologies for the pretreatment of lignocellulosic materials for bio-based products. *Appl. Microbiol. Biotechnol.* **104**, 455–473 (2020).
11. N. Mosier, C. Wyman, B. Dale, R. Elander, Y. Y. Lee, M. Holtzapple, M. Ladisch, Features of promising technologies for pretreatment of lignocellulosic biomass. *Bioresour. Technol.* **96**, 673–686 (2005).
12. J. T. Cunha, A. Romaní, C. E. Costa, I. Sá-Correia, L. Domingues, Molecular and physiological basis of *Saccharomyces cerevisiae* tolerance to adverse lignocellulose-based process conditions. *Appl. Microbiol. Biotechnol.* **103**, 159–175 (2019).
13. F. K. Kazi, J. A. Fortman, R. P. Anex, D. D. Hsu, A. Aden, A. Dutta, G. Kothandaraman, Techno-economic comparison of process technologies for biochemical ethanol production from corn stover. *Fuel* **89**, S20–S28 (2010).
14. J. K. Ko, Y. Um, Y.-C. Park, J.-H. Seo, K. H. Kim, Compounds inhibiting the bioconversion of hydrothermally pretreated lignocellulose. *Appl. Microbiol. Biotechnol.* **99**, 4201–4212 (2015).
15. J. R. Almeida, T. Modig, A. Petersson, B. Hahn-Hägerdal, G. Lidén, M. F. Gorwa-Grauslund, Increased tolerance and conversion of inhibitors in lignocellulosic hydrolysates by *Saccharomyces cerevisiae*. *J. Chem. Technol. Biotechnol.* **82**, 340–349 (2007).
16. F. H. Lam, A. Ghaderi, G. R. Fink, G. Stephanopoulos, Engineering alcohol tolerance in yeast. *Science* **346**, 71–75 (2014).
17. H. B. Klinke, A. B. Thomsen, B. K. Ahring, Inhibition of ethanol-producing yeast and bacteria by degradation products produced during pre-treatment of biomass. *Appl. Microbiol. Biotechnol.* **66**, 10–26 (2004).
18. D. Heer, U. Sauer, Identification of furfural as a key toxin in lignocellulosic hydrolysates and evolution of a tolerant yeast strain. *J. Microbial. Biotechnol.* **1**, 497–506 (2008).
19. Y. H. Jung, I. J. Kim, H. K. Kim, K. H. Kim, Dilute acid pretreatment of lignocellulose for whole slurry ethanol fermentation. *Bioresour. Technol.* **132**, 109–114 (2013).
20. E. Palmqvist, B. Hahn-Hägerdal, Fermentation of lignocellulosic hydrolysates. II: Inhibitors and mechanisms of inhibition. *Bioresour. Technol.* **74**, 25–33 (2000).
21. S. Larsson, E. Palmqvist, B. Hahn-Hägerdal, C. Tengborg, K. Stenberg, G. Zacchi, N.-O. Nilvebrant, The generation of fermentation inhibitors during dilute acid hydrolysis of softwood. *Enzyme Microb. Technol.* **24**, 151–159 (1999).
22. T. Y. Mills, N. R. Sandoval, R. T. Gill, Cellulosic hydrolysate toxicity and tolerance mechanisms in *Escherichia coli*. *Biotechnol. Biofuels* **2**, 26 (2009).
23. M. P. Almario, L. H. Reyes, K. C. Kao, Evolutionary engineering of *Saccharomyces cerevisiae* for enhanced tolerance to hydrolysates of lignocellulosic biomass. *Biotechnol. Bioeng.* **110**, 2616–2623 (2013).
24. C. B. Brachmann, A. Davies, G. J. Cost, E. Caputo, J. Li, P. Hieter, J. D. Boeke, Designer deletion strains derived from *Saccharomyces cerevisiae* S288C: A useful set of strains and plasmids for PCR-mediated gene disruption and other applications. *Yeast* **14**, 115–132 (1998).
25. S. A. Allen, W. Clark, J. M. McCaffery, Z. Cai, A. Lanctot, P. J. Slininger, Z. L. Liu, S. W. Gorsich, Furfural induces reactive oxygen species accumulation and cellular damage in *Saccharomyces cerevisiae*. *Biotechnol. Biofuels* **3**, 2 (2010).
26. E. Casey, M. Sedlak, N. W. Y. Ho, N. S. Mosier, Effect of acetic acid and pH on the cofermentation of glucose and xylose to ethanol by a genetically engineered strain of *Saccharomyces cerevisiae*. *FEMS Yeast Res.* **10**, 385–393 (2010).
27. M. J. Taherzadeh, L. Gustafsson, C. Niklasson, G. Lidén, Conversion of furfural in aerobic and anaerobic batch fermentation of glucose by *Saccharomyces cerevisiae*. *J. Biosci. Bioeng.* **87**, 169–174 (1999).
28. J. R. M. Almeida, A. Röder, T. Modig, B. Laadan, G. Lidén, M. F. Gorwa-Grauslund, NADH- vs NADPH-coupled reduction of 5-hydroxymethyl furfural (HMF) and its implications on product distribution in *Saccharomyces cerevisiae*. *Appl. Microbiol. Biotechnol.* **78**, 939–945 (2008).
29. D. Heer, D. Heine, U. Sauer, Resistance of *Saccharomyces cerevisiae* to high concentrations of furfural is based on NADPH-dependent reduction by at least two oxireductases. *Appl. Environ. Microbiol.* **75**, 7631–7638 (2009).
30. Z. Lewis Liu, J. Moon, B. J. Andersh, P. J. Slininger, S. Weber, Multiple gene-mediated NAD(P)H-dependent aldehyde reduction is a mechanism of in situ detoxification of furfural and 5-hydroxymethylfurfural by *Saccharomyces cerevisiae*. *Appl. Microbiol. Biotechnol.* **81**, 743–753 (2008).
31. J. Moon, Z. L. Liu, Engineered NADH-dependent GRE2 from *Saccharomyces cerevisiae* by directed enzyme evolution enhances HMF reduction using additional cofactor NADPH. *Enzyme Microb. Technol.* **50**, 115–120 (2012).
32. A. Petersson, J. R. M. Almeida, T. Modig, K. Karhumaa, B. Hahn-Hägerdal, M. F. Gorwa-Grauslund, G. Lidén, A 5-hydroxymethyl furfural reducing enzyme encoded by the *Saccharomyces cerevisiae* ADH6 gene conveys HMF tolerance. *Yeast* **23**, 455–464 (2006).
33. M. Ma, X. Wang, X. Zhang, X. Zhao, Alcohol dehydrogenases from *Scheffersomyces stipitis* involved in the detoxification of aldehyde inhibitors derived from lignocellulosic biomass conversion. *Appl. Microbiol. Biotechnol.* **97**, 8411–8425 (2013).
34. E. R. Jerison, A. N. Nguyen Ba, M. M. Desai, S. Kryazhimskiy, Chance and necessity in the pleiotropic consequences of adaptation for budding yeast. *Nat. Ecol. Evol.* **4**, 601–611 (2020).
35. W. Qian, D. Ma, C. Xiao, Z. Wang, J. Zhang, The genomic landscape and evolutionary resolution of antagonistic pleiotropy in yeast. *Cell Rep.* **2**, 1399–1410 (2012).
36. Z. Huang, K. Chen, J. Zhang, Y. Li, H. Wang, D. Cui, J. Tang, Y. Liu, X. Shi, W. Li, D. Liu, R. Chen, R. S. Sucgang, X. Pan, A functional variomics tool for discovering drug-resistance genes and drug targets. *Cell Rep.* **3**, 577–585 (2013).
37. S. H. Mohd Azhar, R. Abdulla, S. A. Jambo, H. Marbawi, J. A. Gansau, A. A. Mohd Faik, K. F. Rodrigues, Yeasts in sustainable bioethanol production: A review. *Biochem. Biophys. Rep.* **10**, 52–61 (2017).
38. X. Chen, E. Kuhn, E. W. Jennings, R. Nelson, L. Tao, M. Zhang, M. P. Tucker, DMR (deacetylation and mechanical refining) processing of corn stover achieves high monomeric sugar concentrations (230 g L^{-1}) during enzymatic hydrolysis and high ethanol concentrations (>10% v/v) during fermentation without hydrolysate purification or concentration. *Energ. Environ. Sci.* **9**, 1237–1245 (2016).
39. L. Tao, D. Schell, R. Davis, E. Tan, R. Elander, A. Bratis, "NREL 2012 achievement of ethanol cost targets: Biochemical ethanol fermentation via dilute-acid pretreatment and enzymatic hydrolysis of corn stover" (Technical Report NREL/TP-5100-61563, 1129271, 2014).
40. B. Zhang, H. Sun, J. Li, Y. Wan, Y. Li, Y. Zhang, High-titer-ethanol production from cellulosic hydrolysate by an engineered strain of *Saccharomyces cerevisiae* during an in situ removal process reducing the inhibition of ethanol on xylose metabolism. *Process Biochem.* **51**, 967–972 (2016).
41. M. W. Lau, B. E. Dale, Cellulosic ethanol production from AFEX-treated corn stover using *Saccharomyces cerevisiae* 424A(LNH-ST). *Proc. Natl. Acad. Sci. U.S.A.* **106**, 1368–1373 (2009).
42. X. Liu, H. Liu, P. Yan, L. Mao, Z. Xu, Z. C. Zhang, Mechanocatalytic synergy for expedited cellulosic ethanol production compatible with integrated biorefinery. *ACS Sustain. Chem. Eng.* **8**, 2399–2408 (2020).
43. S. M. O'Rourke, I. Herskowitz, Unique and redundant roles for HOG MAPK pathway components as revealed by whole-genome expression analysis. *Mol. Biol. Cell* **15**, 532–542 (2004).
44. J. C. Varela, C. van Beekvelt, R. J. Planta, W. H. Mager, Osmostress-induced changes in yeast gene expression. *Mol. Microbiol.* **6**, 2183–2190 (1992).
45. A. P. Capaldi, T. Kaplan, Y. Liu, N. Habib, A. Regev, N. Friedman, E. K. O'Shea, Structure and function of a transcriptional network activated by the MAPK Hog1. *Nat. Genet.* **40**, 1300–1306 (2008).
46. H. Zhou, J.-S. Cheng, B. L. Wang, G. R. Fink, G. Stephanopoulos, Xylose isomerase overexpression along with engineering of the pentose phosphate pathway and evolutionary engineering enable rapid xylose utilization and ethanol production by *Saccharomyces cerevisiae*. *Metab. Eng.* **14**, 611–622 (2012).
47. Global lactic acid market size & share report, 2019–2025 (2021); www.grandviewresearch.com/industry-analysis/lactic-acid-and-poly-lactic-acid-market.
48. D. A. Abbott, R. M. Zelle, J. T. Pronk, A. J. A. van Maris, Metabolic engineering of *Saccharomyces cerevisiae* for production of carboxylic acids: Current status and challenges. *FEMS Yeast Res.* **9**, 1123–1136 (2009).
49. M. T. Flikweert, L. Van Der Zanden, W. M. Janssen, H. Y. Steensma, J. P. van Dijken, J. T. Pronk, Pyruvate decarboxylase: An indispensable enzyme for growth of *Saccharomyces cerevisiae* on glucose. *Yeast* **12**, 247–257 (1996).
50. H. Alper, C. Fischer, E. Nevoigt, G. Stephanopoulos, Tuning genetic control through promoter engineering. *Proc. Natl. Acad. Sci. U.S.A.* **102**, 12678–12683 (2005).
51. S. Hohmann, Characterization of PDC6, a third structural gene for pyruvate decarboxylase in *Saccharomyces cerevisiae*. *J. Bacteriol.* **173**, 7963–7969 (1991).
52. S.-H. Baek, E. Y. Kwon, Y. H. Kim, J.-S. Hahn, Metabolic engineering and adaptive evolution for efficient production of D-lactic acid in *Saccharomyces cerevisiae*. *Appl. Microbiol. Biotechnol.* **100**, 2737–2748 (2016).
53. T. L. Turner, G.-C. Zhang, E. J. Oh, V. Subramaniam, A. Adiputra, V. Subramaniam, C. D. Skory, J. Y. Jang, B. J. Yu, I. Park, Y.-S. Jin, Lactic acid production from cellobiose and xylose by engineered *Saccharomyces cerevisiae*. *Biotechnol. Bioeng.* **113**, 1075–1083 (2016).
54. N. Ishida, S. Saitoh, T. Onishi, K. Tokuhiro, E. Nagamori, K. Kitamoto, H. Takahashi, The effect of pyruvate decarboxylase gene knockout in *Saccharomyces cerevisiaeon* L-lactic acid production. *Biosci. Biotechnol. Biochem.* **70**, 1148–1153 (2006).
55. A. L. Walter, D. Yang, Z. Zeng, D. Bayrock, P. E. Urriola, G. C. Shurson, Assessment of antibiotic resistance from long-term bacterial exposure to antibiotics commonly used in fuel ethanol production. *World J. Microbiol. Biotechnol.* **35**, 66 (2019).
56. D. Mumberg, R. Müller, M. Funk, Yeast vectors for the controlled expression of heterologous proteins in different genetic backgrounds. *Gene* **156**, 119–122 (1995).

57. R. D. Gietz, R. H. Schiestl, A. R. Willems, R. A. Woods, Studies on the transformation of intact yeast cells by the LiAc/SS-DNA/PEG procedure. *Yeast* **11**, 355–360 (1995).
58. I. Herskowitz, R. E. Jensen, [8] Putting the *HO* gene to work: Practical uses for mating-type switching. *Meth. Enzymol.* **194**, 132–146 (1991).
59. G. F. Sprague Jr., [5] Assay of yeast mating reaction. *Meth. Enzymol.* **194**, 77–93 (1991).
60. V. K. Vyas, M. I. Barrasa, G. R. Fink, A *Candida albicans* CRISPR system permits genetic engineering of essential genes and gene families. *Sci. Adv.* **1**, e1500248 (2015).
61. M. P. Tucker, "High titer and yields achieved with novel, low-severity pretreatment strategy" (2016); www.nrel.gov/docs/fy16osti/65917.pdf.

Acknowledgments: We extend appreciation to various members of the Whitehead Institute and MIT Department of Chemical Engineering: V. Vyas and B. Uranukul for broad-ranging discussions and technical feedback; C. Ni and K. Fox for chromatography expertise; S. Rajavasireddy, M. Torrens-Spence, J. Morgan, J. Park, and N. Liu for technical assistance; and B. Chan and C. Lewis at the Whitehead Institute Metabolite Profiling Core Facility for running metabolomics samples and data analysis. Additional thanks go to partners who provided critical material or testing services: D. Peterson (U.S. National Renewable Energy Laboratory); S. Bauer (U.S. Lawrence Berkeley National Laboratory); J. Caupert, S. Trupia, and A. Athmanathan (National Corn-to-Ethanol Research Center); R. Reeves and G. Doherty (Ethtec); P. Ferrando (Versalis Biochemtex); and M. Smith (Environmental Testing and Research Laboratories). We also thank D. Babson, I. Rowe, and C. Rohman at the U.S. Department of Energy (DOE) for grant management support and insight into energy policy. **Funding:** This work was supported by award number DE-EE0007531 to G.S. from the DOE Office of Energy Efficiency and Renewable Energy (EERE) under the Bioenergy Technologies Office (BETO). Additional funding provided by NIH grant R01-GM035010 to G.R.F. B.T.-Y. supported partly by The Scientific and Technological Research Council of Turkey (TUBITAK) International Postdoctoral Research Fellowship Programme. This work also authored in part by the National Renewable Energy Laboratory, operated by Alliance for Sustainable Energy LLC, for the DOE under contract number DE-AC36-08GO28308 provided by EERE BETO. The views expressed in the article do not necessarily represent the views of the DOE or U.S. government. The U.S. government retains and the publisher, by accepting the article for publication, acknowledges that the U.S. government retains a nonexclusive, paid-up, irrevocable, and worldwide license to publish or reproduce the published form of this work, or allow others to do so, for U.S. government purposes. **Author contributions:** F.H.L., G.R.F., and G.S. cowrote the manuscript. B.T.-Y. conducted early characterization studies. D.L. assisted with fermentations. M.G.R. provided critical material. F.H.L. conceived all experiments and performed all reagent construction, remaining experiments, and analyses of data. **Competing interests:** F.H.L., G.R.F., and G.S. are listed as coinventors on a provisional patent filed by MIT and the Whitehead Institute. All other authors declare that they have no other competing interests. **Data and materials availability:** All data needed to evaluate the conclusions in the paper are present in the paper and/or the Supplementary Materials. Corn stover–derived hydrolysates can be provided by the U.S. National Renewable Energy Laboratory pending scientific review and a completed material transfer agreement. Requests should be directed to M.G.R. Wheat straw hydrolysate can be provided by Versalis (Eni) pending a similar review and agreement. Inquiries should be submitted to info.licensing@versalis.eni.com. Correspondence and requests for strains, plasmids, and other materials can be addressed to G.S. or G.R.F. Additional data related to this paper may be requested from the authors.

Submitted 18 November 2020
Accepted 13 May 2021
Published 25 June 2021
10.1126/sciadv.abf7613

Citation: F. H. Lam, B. Turanlı-Yıldız, D. Liu, M. G. Resch, G. R. Fink, G. Stephanopoulos, Engineered yeast tolerance enables efficient production from toxified lignocellulosic feedstocks. *Sci. Adv.* **7**, eabf7613 (2021).

Science Advances

Engineered yeast tolerance enables efficient production from toxified lignocellulosic feedstocks

Felix H. Lam, Burcu Turanli-Yildiz, Dany Liu, Michael G. Resch, Gerald R. Fink and Gregory Stephanopoulos

Sci Adv **7** (26), eabf7613.
DOI: 10.1126/sciadv.abf7613